nature catalysis

ARTICLES

https://doi.org/10.1038/s41929-019-0230-x

Asymmetric formation of γ-lactams via C–H amidation enabled by chiral hydrogen-bond-donor catalysts

Yoonsu Park[1,2] and Sukbok Chang[1,2*]

Chiral γ-lactams are effective structural motifs found in numerous pharmaceutical agents. Despite their importance, current approaches mostly necessitate laborious synthetic steps employing pre-functionalized starting materials under demanding conditions. In this regard, asymmetric C–H amidation can provide an ideal platform for rapid construction of this valuable scaffold from unactivated materials, but unsolved issues have hampered the strategy. Here, we report iridium catalysts that overcome these challenges by utilizing chiral hydrogen-bond-donor ligands. The protocol makes use of easily accessible substrates derived from carboxylic acid, which display excellent efficiency and enantioselectivity towards direct amidation of prochiral sp^3 C–H bonds. Desymmetrization of *meso*-substrates is also achieved, where two consecutive stereogenic centres are selectively introduced in a single transformation. Computational investigations reveal the presence of crucial hydrogen bonding in the stereo-determining transition states and spectroscopic analysis of the structural analogues further corroborate this non-covalent interaction.

Chiral cyclic amides are an important class of molecular scaffolds that exhibit versatile biological activity. Along with the β-lactams that are widely present in ground-breaking antibiotics[1], five-membered lactams with a γ-chiral centre have been recognized as a functional core unit in both natural compounds and effective clinical drugs, including anticancer agents (Fig. 1a)[2]. Although tremendous efforts have been made to develop efficient and selective methods to construct this structural motif[3–5], synthetic challenges to the installation of the chiral centres have impeded their advancement. Classical approaches to chiral γ-lactams mostly rely on laborious derivatization procedures starting from glutamic acids, where harsh reaction conditions limit their utility mainly to early-stage applications[6]. Only recently have a number of asymmetric protocols been developed for the direct construction of the chiral centres. Representative examples include enantioselective cyclization of allyl alcohols[7], hydrogenation of unsaturated lactams[8] and C–H activation of *N*-pyridyl lactams[9]. However, all of these approaches require the pre-installation of multiple functional groups in the substrates, thus diminishing the atom economy and cost efficiency.

Our initial proposal for this problem was that the most efficient way to construct chiral γ-lactams from otherwise unactivated materials would be a direct C–H amidation of acyclic amide derivatives (Fig. 1b). This elusive retrosynthetic route is particularly interesting because the aliphatic amides can be prepared easily from feedstock chemicals such as carboxylic acids and esters. The key technology in this proposition is centred on the asymmetric C–H functionalization reaction[10–12]. In the last two decades, a number of research groups have reported the synthesis of chiral azacyclic compounds such as sulfamidates, sulfonamides and carbamates through C–H amidation reactions (Fig. 1c)[13]. Early findings by the Che group showcased that ruthenium catalysts bearing chiral porphyrins allow enantioselective synthesis of chiral sulfamidates[14]. This first demonstration inspired further developments, and chiral catalysts including dirhodium complexes with amino-acid- or carboxamidate-based ligands[15,16], ruthenium–oxazoline species[17], iridium–metallosalen complexes[18] and engineered metalloenzymes[19–21] have been reported. Despite those efforts, concurrent developments are mostly confined to the cyclization of sulfonyl- or carbamate-based substrates. This is mainly due to the easy accessibility and robustness of the utilized nitrene precursors such as iminoiodinanes and organic azides[13,22–24], and the absence of notable side reaction pathways from highly reactive metal–nitrenoid intermediates. In sharp contrast, asymmetric C–H amidation for chiral lactam synthesis has been elusive so far because of several unsolved issues: (1) robust, but reactive carbonylnitrene precursors are underdeveloped[25], (2) suppression of undesired decomposition of the key metal–nitrenoid intermediates to isocyanates is challenging[26,27] and (3) a stereochemical model for asymmetric induction is poorly understood. Overall, enantioselective construction of chiral lactams remains to be achieved.

We now introduce a new array of organometallic catalysts that overcome those challenges and produce chiral γ-lactams in unprotected forms from acyclic carboxylic acid derivatives (Fig. 1d). Taking advantage of recently developed robust precursors[28], new iridium-based chiral catalysts that can be readily prepared from commercially available ligands have been developed that display excellent reactivity and enantioselectivity through C–H amidation technology. Comprehensive mechanistic investigations indicate that the critical component for excellent stereoselectivity is a transient intramolecular hydrogen bonding that stabilizes key intermediates and transition states selectively.

Results

Reaction design and mechanistic challenges. In 2015, our group reported that 1,4,2-dioxazol-5-one compounds are thermally stable, yet highly reactive nitrene precursors for C–H amidation under pentamethylcyclopentadienyl (Cp*)-based metal catalysis[28,29].

[1]Department of Chemistry, Korea Advanced Institute of Science and Technology (KAIST), Daejeon, Republic of Korea. [2]Center for Catalytic Hydrocarbon Functionalizations, Institute for Basic Science (IBS), Daejeon, Republic of Korea. *e-mail: sbchang@kaist.ac.kr

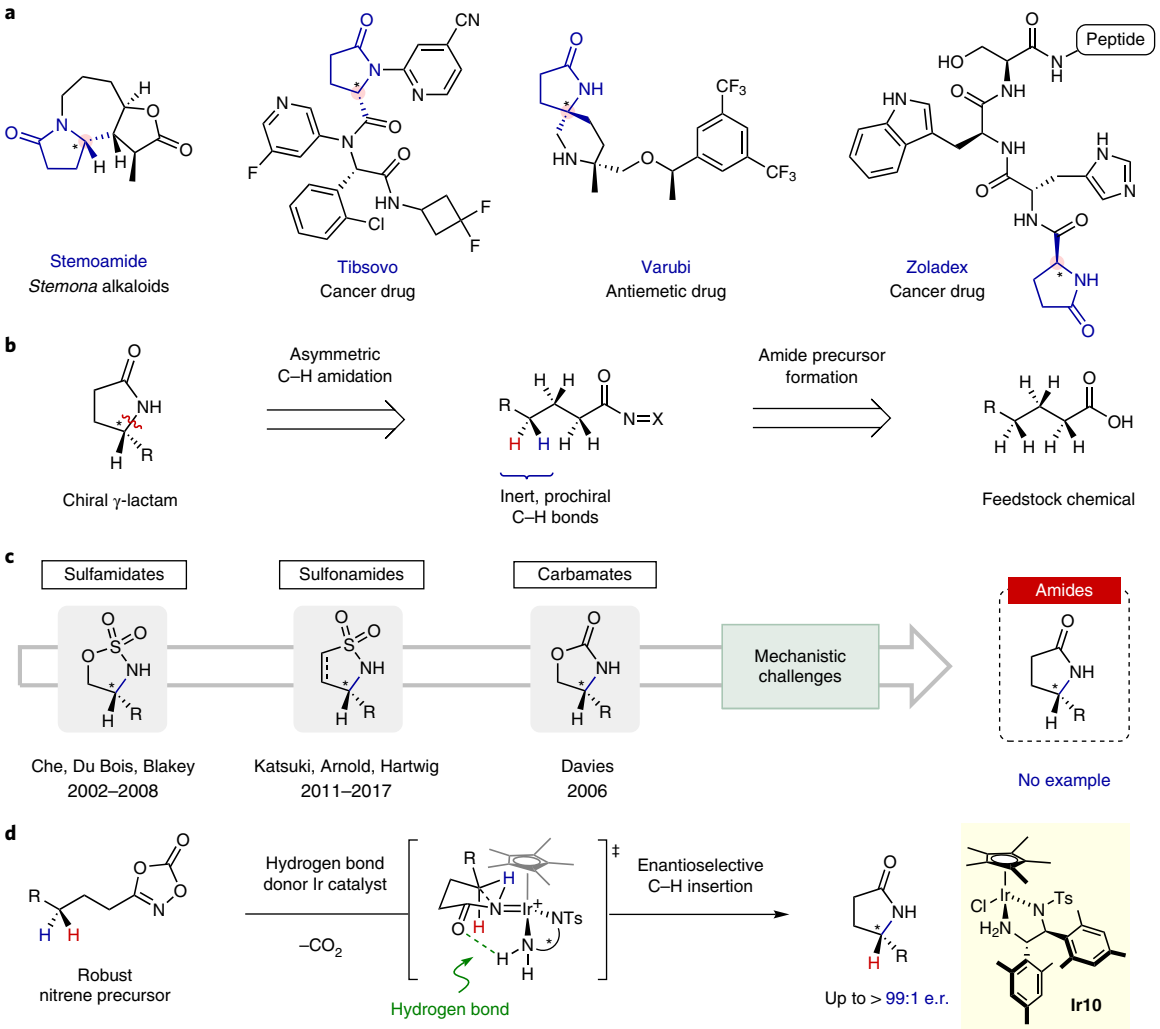

Fig. 1 | Design of an asymmetric C–H amidation for chiral γ-lactam synthesis. a, Naturally occurring alkaloids and clinical drugs with a chiral γ-lactam moiety. **b**, Retrosynthetic proposal for chiral lactam synthesis through C–H functionalization of aliphatic amide derivatives. **c**, Advancement of asymmetric C–H amidation for chiral five-membered azacycle synthesis. Chiral amide formation has been regarded as a challenge due to the mechanistic obstacles. **d**, This work: asymmetric formation of γ-lactams via C–H amidation enabled by hydrogen-bond-donor catalysts.

Based on a number of studies to pinpoint the origin of the reactivity[30,31], we recently elaborated the dioxazolones to construct racemic γ-lactams by introducing bidentate anionic ligands in Cp*Ir(III) catalysts[32]. We envisioned that this technology could be utilized as an effective handle for chiral lactam production by creating a chiral environment at the metal centre. However, significant challenges were found in the asymmetry-inducing processes (Fig. 2).

In our previous report[32], we proposed that the first step to enter the catalytic cycle is the formation of a substrate-bound adduct species **B** from the coordinatively unsaturated 16-electron complex **A**. Four distinctive diastereomers are possible on binding of the substrate to the chiral catalysts, where each conformation might lead to different stereochemical outcomes. While this first step does not determine the enantioselectivity, a diastereoselective coordination is necessary to reduce the number of accessible intermediates and transition states (vide infra). The selective complexation would then induce a facile decarboxylation from the corresponding diastereomeric adduct to give an Ir–carbonylnitrenoid species **C**, which is the key intermediate for the subsequent C–H amidation. The sophisticated reactivity control of **C** is another challenge due to the facile Curtius-type deconstruction to undesired isocyanates provoked by its highly electrophilic nature[26,27]. This undesired side pathway needs to be effectively prevented to achieve enantioselective nitrenoid insertion into a prochiral C–H bond. In addition, the resulting chiral amide has a free N–H bond, which could potentially lead to product inhibition or catalyst poisoning[33].

Reaction development. Based on the above mechanistic considerations, we designed and prepared a set of catalysts bearing chiral anionic donors, as shown in Table 1. We initially sought to test *N*,*O*- and *N*,*N*′-bidentate chiral ligands, which might effectively suppress the Curtius-type rearrangement based on our previous observation[32]. Common *N*,*O* donors, such as amino acids (**Ir1**, **Ir2**) and amino alcohols (**Ir3**), were devised as potential candidates for the chiral ligand. D-Prolinamide (**Ir4**), an *N*,*N*′ donor analogue of proline, and chiral diamines (**Ir5**, **Ir6**) that were highly effective for the previous asymmetric transfer hydrogenation reactions[34] were also chosen for the initial assessment.

At the outset, the reactivity and selectivity towards asymmetric C–H amidation were evaluated by subjecting catalytic amounts of chiral iridium complexes and sodium organoborate into a solution of a model substrate **1** in 1,1,2,2-tetrachloroethane-d_2. Formation of the desired product **2** was indeed observed with the *N*,*O*-dentating catalysts, but only in low levels of enantioselectivity along with the

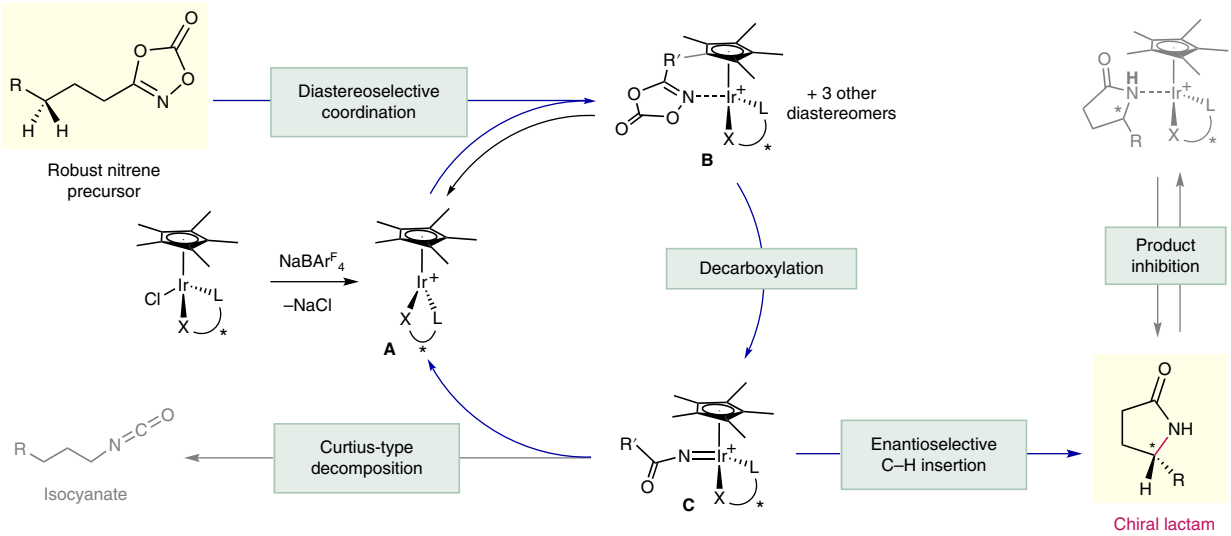

Fig. 2 | Mechanistic challenges based on potential reaction working modes. Blue lines indicate potential productive pathways for asymmetric C–H amidation. Grey lines and structures represent off-cycle pathways and species, respectively.

Table 1 | Catalyst development of iridium-catalysed asymmetric C–H amidation

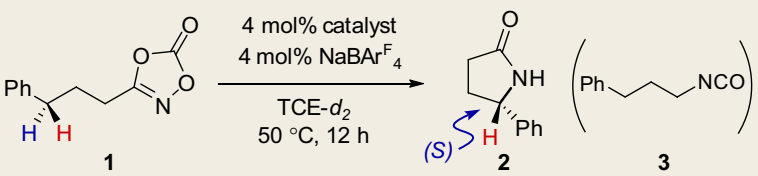

Entry	Catalyst	Yield of **2** (%)	e.r. of **2**	Yield of **3** (%)
1	**Ir1**	19	53:47	28
2	**Ir2**	24	51:49	24
3	**Ir3**	39	51:49	22
4	**Ir4**	40	59:41	35
5	**Ir5**	19	87:13	5
6	**Ir6**	31	98:2	<5
7	**Ir7**	25	91:9	<5
8	**Ir8**	19	94:6	<5
9	**Ir9**	12	96:4	<5
10	**Ir10**	>95	98:2	<5
11[a]	**Ir10**	>95 (96[b])	>99:1	<5
12[c]	**Ir10**	<5	-	73

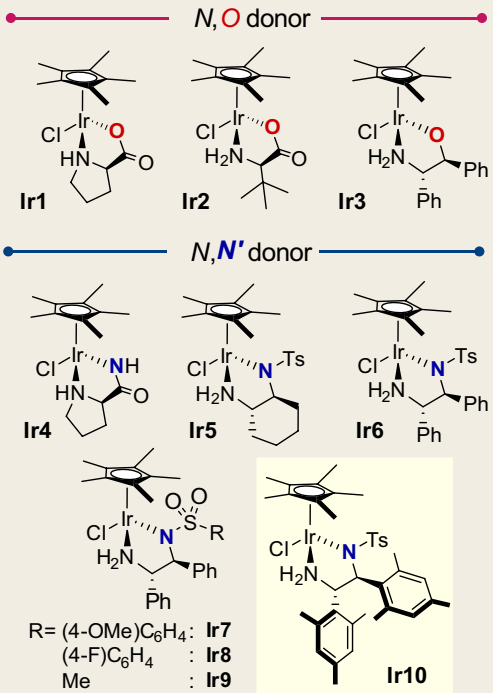

Conditions: **1** (0.1 mmol), catalyst (4 mol%) and sodium tetrakis(3,5-bis(trifluoromethyl)phenyl)borate (NaBAr$^F_4$, 4 mol%) in 1,1,2,2-tetrachloroethane-d_2 (TCE-d_2, 0.5 ml) at 50 °C for 12 h. Yields were determined by ^{1}H NMR analysis using 1,1,2-trichloroethane as an internal standard. Values of e.r. were determined by HPLC analysis. [a]Run at 35 °C for 24 h. [b]Isolated yield. [c]Without NaBAr$^F_4$.

significant formation of the undesired isocyanate **3** (entries 1–3). In sharp contrast, *N*,*N*′-donors suppressed the side pathway more effectively and, to our delight, dramatic increases in enantioselectivity were achieved with the chiral diamine scaffolds. For instance, the diamine catalyst bearing (1*S*,2*S*)-1,2-diaminocyclohexane (**Ir5**) gave chiral **2** in 87:13 e.r. (entry 5). An excellent enantioselectivity was observed using *N*-protected diphenylethylenediamine catalyst (**Ir6**) along with a complete suppression of the isocyanate formation (98:2 e.r., entry 6). Motivated by these initial findings, we also synthesized derivatives of **Ir6** to interrogate structural impacts on the catalytic performance. While perturbation on the *N*-sulfonyl group did not give a notable improvement in product yields (entries 7–9), replacing the phenyl moieties on the ethylene backbone with dimesityl groups (**Ir10**) dramatically enhanced the product yield (>95%) without erosion of the stereochemical fidelity. The increase in product yield might be understood as a beneficial effect of mesityl groups to preclude product inhibition or catalyst decomposition, as discussed in the Supplementary Discussion. The absolute configuration of **2** was determined as (*S*) by comparing the optical rotation with reported values[35]. Further evaluation of the reaction

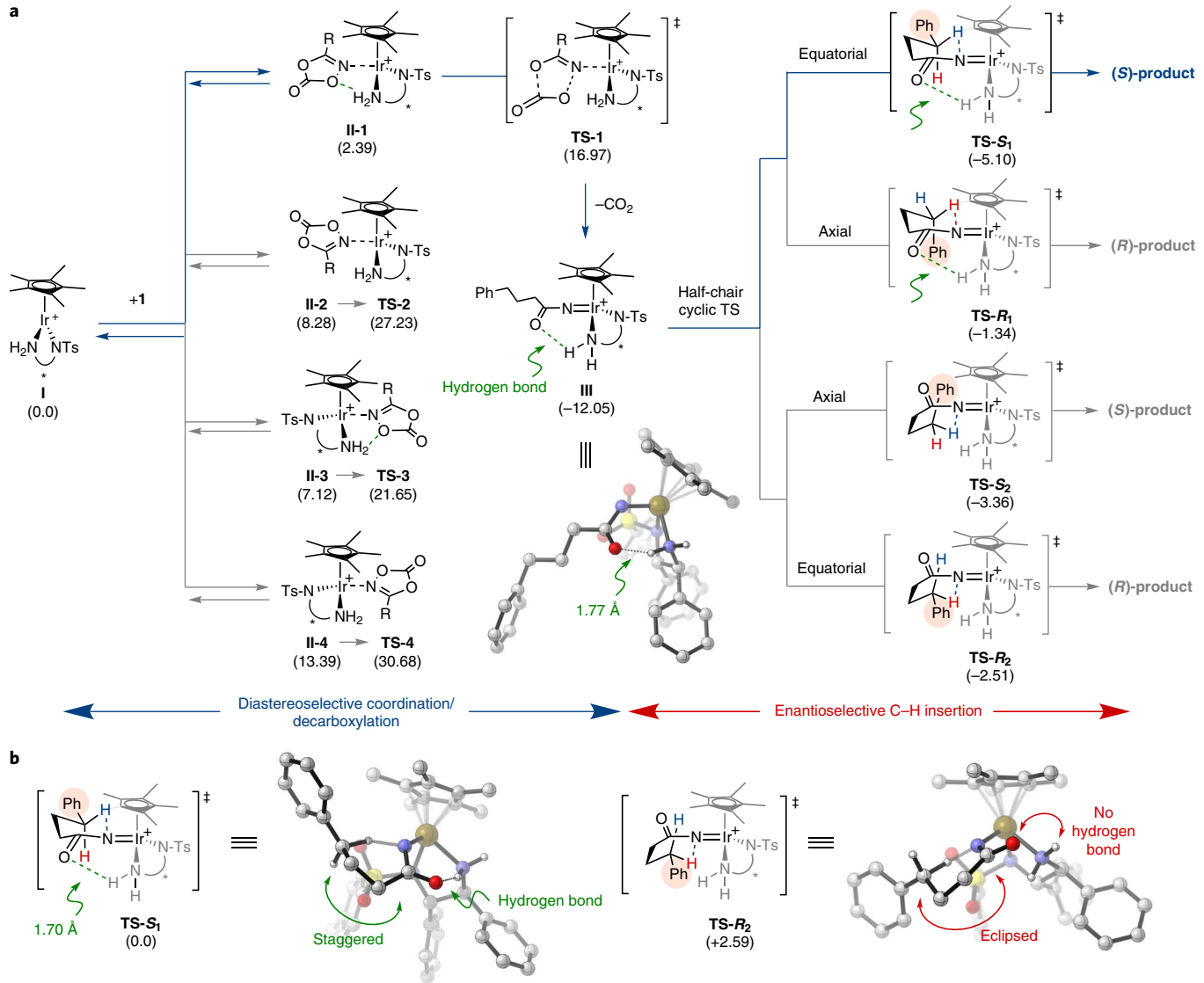

Fig. 3 | Stereochemical model based on DFT calculations for the asymmetric C–H amidation. a, Possible reaction pathways and their free energy profile at the PCM (dichloroethane) M06/{SDD, 6-311+G(d,p)}//B3LYP/{LANL2DZ, 6-31G(d,p)} level of theory. Blue lines represent the most favoured pathway. R, C_3H_6Ph. Cartesian coordinates for the optimized structures are provided in Supplementary Data 1. **b**, Computed transition state structures for the enantioselective C–H insertion step and their relative free energies with respect to **TS-S_1**. TS, transition state.

parameters, including temperature, time and solvent, resulted in the optimal conditions to afford **2** in 96% isolated yield and >99:1 e.r. (entries 11 and 12 and Supplementary Table 5). Notably, a sharp decrease in enantioselectivity was observed when polar protic solvents such as ethanol, trifluoroethanol and hexafluoroisopropanol were used, suggesting the potential involvement of a non-covalent interaction during the asymmetric catalysis (vide infra). It is worth noting here that the diamine ligands are commercially available, highlighting the easy accessibility of our new catalyst.

Stereochemical origin of the enantioselectivity. Considering the presupposed mechanism in Fig. 2, it was surprising to see that catalyst **Ir10** overcame the various mechanistic challenges and displayed such high enantioselectivity. We therefore sought to understand how the chiral diamine scaffold enables C–H bond amidation with such stereoselectivity. Our particular goal was to establish a stereochemical model to show how (*S*)-configured lactam **2** is selectively formed. To evaluate the kinetic accessibility of the possible states, density functional theory (DFT) calculations were performed for the potential reaction pathways, and the results are displayed in Fig. 3. Because enantiomeric ratios obtained with catalysts **Ir6** and **Ir10** were essentially same, the structure of complex **Ir6** was utilized in mechanistic studies to reduce the computational and experimental costs.

We hypothesized that a prerequisite for selective C–H insertion would be predominant generation of diastereomeric adduct and carbonylnitrenoid species. Interestingly, quantum chemical calculations reveal notable thermodynamic differences between four possible diastereomeric adduct species: chiral (1*S*, 2*S*) diamine ligand makes complex **II-1**, with the (*S*)-configuration at the metal centre, as the most stable conformer[36], while (*R*)-configured **II-4** is destabilized by 11 kcal mol^{-1} more than **II-1**. Another (*S*)-configured diastereomer, **II-2**, is higher in energy than the analogous **II-1** by 5.9 kcal mol^{-1}, and this difference is probably a consequence of interaction between the 1*O* atom of 1,4,2-dioxazol-5-one and the ligand, as shown in the optimized geometries in Supplementary Fig. 34. While the 1*O* moiety shows a repulsive interaction with the Ts group in **II-2**, a weak hydrogen bonding between the 1*O* atom

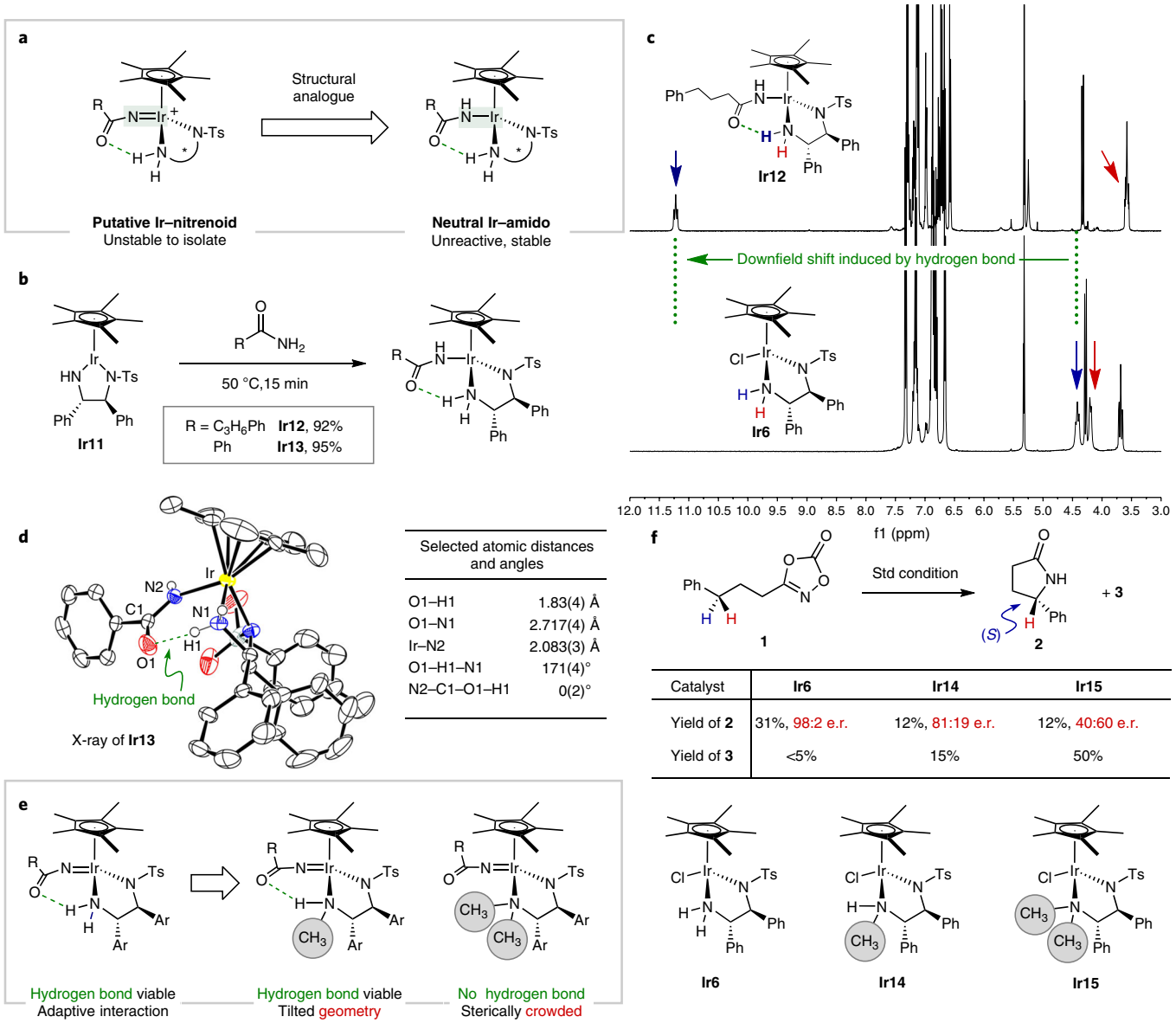

Fig. 4 | Experimental investigation of the intramolecular hydrogen bond between substrate and catalysts. a, A strategy to interrogate the structural signatures of putative Ir–nitrenoid species with analogous Ir–amido complexes. **b**, Synthesis of Ir–amido complexes **Ir12** and **Ir13**. **c**, ^{1}H NMR spectra of **Ir12** (top) and **Ir6** (bottom). Blue and red peaks are assigned to the respective protons in the N–H moieties. **d**, Solid-state structure of **Ir13**. Values in parentheses indicate standard deviations. **e**, A strategy to study the impact of hydrogen bond strength with modified catalysts. **f**, Catalytic performances with *N*-methylated catalysts **Ir14** and **Ir15**. Standard conditions: **1** (0.1 mmol), catalyst (4 mol%) and $NaBAr^F_4$ (4 mol%) in TCE-d_2 (0.5 ml) at 50 °C for 12 h.

and the N–H hydrogen of the catalyst was observed in **II-1** with an atomic distance of 2.0 Å. Interestingly, this thermodynamic stability of **II-1** further leads to facile decarboxylation by traversing transition state **TS-1** with 17 kcal mol^{-1} of overall reaction barrier and affords the Ir–carbonylnitrenoid complex **III**. On the other hand, as fully illustrated in Supplementary Fig. 36, decarboxylative transition states from intermediates **II-2**, **II-3** and **II-4** require much higher energy barriers of 27, 22 and 31 kcal mol^{-1} through **TS-2**, **TS-3** and **TS-4**, respectively, suggesting that decarboxylation would be operative selectively from **II-1** in this catalytic system.

The electrophilic nature of singlet **III** subsequently induces a nitrene insertion into a γ-C–H bond through a six-membered half-chaired transition state with determination of absolute stereochemistry. Four distinctive transition states for this C–H insertion step were identified, and the lowest-lying transition states leading to (*S*)- and (*R*)-forms were **TS-S_1** and **TS-R_2**, which required 6.95 and 9.54 kcal mol^{-1} of insertion barriers from **III**, respectively. As shown in Fig. 3b, conformational differences between **TS-S_1** and **TS-R_2** were located on a six-membered ring with staggered- and eclipsed-half-chair forms, respectively. Computation predicted a predominant formation of (*S*)-lactam through this **TS-S_1** by 2.6 kcal mol^{-1} of energy difference, and indeed this value is fully consistent with the experimentally observed enantioselectivity of 99:1 e.r. (2.7 kcal mol^{-1}).

By closely analysing the optimized geometries, we identified intramolecular hydrogen bonding interactions between the catalyst and the substrate in a few key structures. As highlighted in Fig. 3a, a putative nitrenoid intermediate **III** clearly displayed a hydrogen

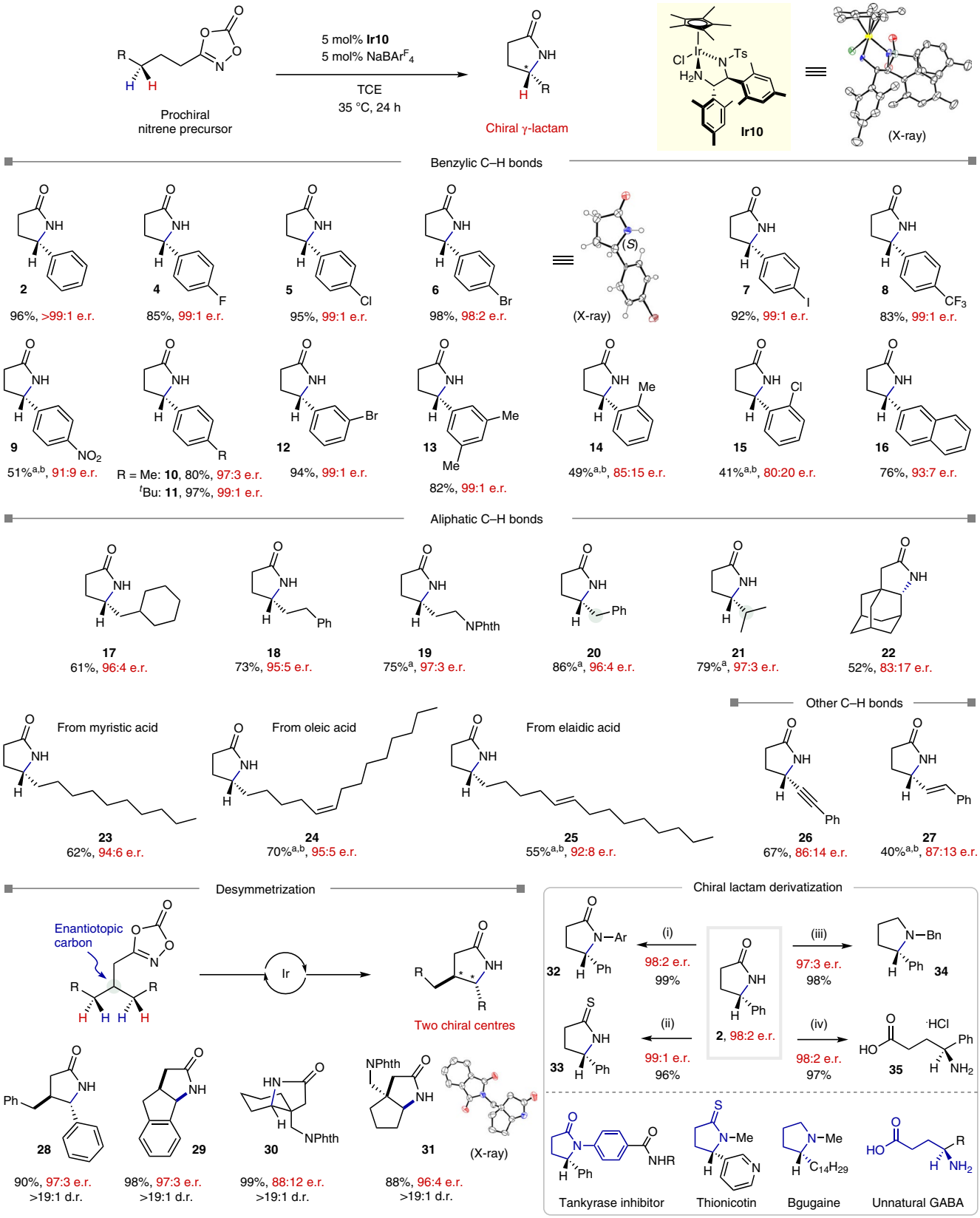

Fig. 5 | Substrate scope and subsequent elaboration from obtained chiral lactams. Conditions: substrate (0.2 mmol), **Ir10** (5 mol%) and NaBAr$^F_4$ (5 mol%) in TCE (1.0 ml) at 35 °C for 24 h. Isolated yields were determined after flash chromatography. Values of e.r. were determined by HPLC analysis. [a]Run at 50 °C. [b]10 mol% of **Ir10** and NaBAr$^F_4$ were used. NPhth, phthalimide. (i) **2** (0.24 mmol), 4-bromobenzonitrile (0.2 mmol), $Pd_2(dba)_3$ (5 mol%), Xantphos (15 mol%) and Cs_2CO_3 (0.28 mmol) in 1,4-dioxane at 105 °C for 12 h. Ar, (*p*-CN)C_6H_4. (ii) **2** (0.1 mmol) and Lawesson's reagent (0.05 mmol) in toluene at 80 °C for 6 h. (iii) **2** (0.1 mmol), benzyl bromide (0.12 mmol) and NaH (0.15 mmol) in tetrahydrofuran at 25 °C for 24 h, then $LiAlH_4$ (0.5 mmol) in tetrahydrofuran at 25 °C for 6 h. (iv) **2** (0.1 mmol) in 6 N HCl at 100 °C for 12 h. GABA, γ-aminobutanoic acid. See Supplementary Methods for experimental details.

bond between the amide oxygen and N–H hydrogen of the catalyst, with an atomic distance of 1.8 Å. Moreover, as shown in Fig. 3b, this interaction is much amplified in the C–H insertion transition state (**TS-S_1**), with a hydrogen bond distance of 1.7 Å, implying that this non-covalent interaction would be closely related to the stereochemical outcomes. In sharp contrast, **TS-R_2** does not have this extra interaction, which rather tilts the amide moiety upwards to release the steric congestion with the Cp* fragment. Thus, the computational analysis led us to conclude that the intramolecular hydrogen bonding might be operative only in **TS-S_1**, eventually making the (*S*)-configured lactam in a more selective manner.

Experimental evidence for the hydrogen bonding interaction. Intrigued by the computational insight into the hydrogen bonding in key steps, we further sought to validate this with experimental support. Although spectroscopic observation of the supposed hydrogen bond in **III** is most compelling, this species was predicted to easily undergo an intramolecular C–H insertion with a kinetic barrier of only 7 kcal mol^{-1} according to the DFT calculations (Fig. 3a), suggesting that its detection might be very challenging. We thus devised a catalytically inactive, yet structurally analogous complex that allows an interrogation of the geometric signatures of **III**. We proposed that the neutral Ir–amido complexes in Fig. 4a would be suitable for this purpose because of the similarity in the coordination environment to **III**. Indeed, the computationally optimized geometry of the Ir–amido species in Supplementary Fig. 35 clearly contained an analogous hydrogen bond, as expected.

Based on this hypothesis, we attempted to synthesize such complexes utilizing reported procedures. Inspired by previous protocols[37,38], the targeted Ir–amido complexes **Ir12** and **Ir13** were successfully synthesized from a 16-electron complex **Ir11** (Fig. 4b). ^{1}H NMR analysis clearly showed the formation of a single diastereomeric adduct and also the presence of intramolecular hydrogen bonding in solution phase, as witnessed by a significant downfield shift of an amine N–H bond (Fig. 4c). The solid-state geometry of **Ir13** further confirmed the viability of the hydrogen bond (Fig. 4d, Supplementary Table 4 and Supplementary Note 2), with the atomic distances and angles between the hydrogen donor and acceptor indicating a two-centred, medium-strength hydrogen bonding[39]. This observation suggested that the Ir–nitrenoid **III** might also display similar interactions as the analogous **Ir12**.

In addition to this structural evidence, the involvement of a hydrogen bond in our catalytic reaction was further evaluated with modified catalysts (Fig. 4e). Because the hydrogen bond strength might be altered upon derivatization of the parent amino group of the catalysts[40], we predicted that *N*-alkylation of the ligand would result in significant erosion of the enantioselectivity. We therefore prepared mono- and di-methylated Ir catalysts to assess the direct impact of the N–H moieties. Indeed, catalysts **Ir14** and **Ir15** afforded lactam **2** in significantly decreased enantioselectivities (81:19 and 40:60 e.r.) compared to the reaction with the parent catalyst (**Ir6**, Fig. 4f). This result clearly demonstrates that the stereo-determining process is critically influenced by the supposed intramolecular hydrogen bond. Of note, an extra steric influence created by dimethyl substitution in **Ir15** presumably resulted in inversion of the absolute configuration.

Substrate scope and utility of the method. We subsequently explored the general applicability of our approach to various types of substrate (Fig. 5). Robust carbonylnitrene precursors, 3-substituted 1,4,2-dioxazol-5-ones, were prepared readily from the corresponding carboxylic acids in two steps with high efficiency. A series of 3-arylpropyl dioxazolones were first examined under the optimized conditions using **Ir10**. The corresponding chiral lactam products were obtained in high yields and excellent enantioselectivities up to >99:1 e.r. Functional group tolerance was observed to be high, including for various substituents such as fluoro, chloro, bromo and iodo groups, without much affecting the stereochemical outcomes (**4**–**7**). The absolute configuration of **6** was further confirmed as the (*S*)-isomer by X-ray analysis, with an absolute structure parameter of 0.04 (Supplementary Table 1)[41]. While electron-deficient trifluoromethyl (**8**) and donating methyl or *tert*-butyl substituents (**10**, **11**) gave rise to excellent results, reductions in reactivity and enantioselectivity were observed with a nitro group (**9**). Although electronic variation of the aryl moiety did not much affect its benzylic C–H insertion process, the positions of the substituents were found to be more critical for the stereo-outcomes. When methyl or chloro groups are substituted at the *ortho*-position, the e.r. drops to 85:15 or 80:20, respectively (**14**, **15**). An extended π-system, such as the 2-naphthyl moiety, was also successfully applicable to the present catalyst system (**16**). Of note, the reaction is convenient to carry out under air without precautions, and a tenfold larger-scale reaction also gave essentially the same result.

The current approach to γ-lactams could be readily applicable to functionalizing aliphatic secondary C(sp^3)–H bonds with high to excellent enantioselectivity. Dioxazolones bearing 4-cyclohexylbutyl (**17**), 5-phenylpentyl (**18**) and 5-imido (**19**) groups were converted to the corresponding chiral pyrrolidinones with >95:5 e.r. Interestingly, high regioselectivity towards the γ-position was observed even in the presence of potentially more reactive benzylic or tertiary δ-C–H bonds (**20**, **21**). The observed regioselectivity pattern is significantly distinct from the known asymmetric amidation catalysis, where six-membered cyclization at the δ-position is highly efficient[14,16–18,42]. The reaction of a dioxazolone substrate having an adamantyl moiety at the β-position provided an optically enriched γ-lactam (**22**) in moderate yield. Naturally abundant and bioactive fatty acids such as myristic, oleic and elaidic acids were readily converted to the corresponding chiral lactams with a good to high level of stereochemical fidelity (**23**–**25**). Other C–H bonds at the propargylic and allylic positions were also amidated under the present catalytic conditions albeit with moderate enantioselectivities (**26**, **27**).

We next wondered whether our procedure might also be applicable to desymmetrization of *meso*-substrates containing an enantiotopic tertiary- or quaternary-carbon for the production of chiral lactams with two consecutive stereogenic centres in a single transformation[43]. To our delight, a substrate containing four benzylic C–H bonds at the γ-position was effectively desymmetrized with an excellent level of enantioselectivity and diastereoselectivity to afford **28** in high yield. Two sets of equivalent C–H bonds in an indane ring were also selectively distinguished to furnish a tricyclic chiral lactam **29** in excellent yield and enantioselectivity. Moreover, a dioxazolone substrate, easily prepared from a top-selling anti-epileptic drug Neurotin, was successfully subjected to the present catalytic conditions, and quantitatively produced a bicyclic lactam **30** bearing a quaternary chiral carbon centre in moderate enantioselectivity. On the other hand, the stereoselectivity was significantly increased with a cyclopentyl analogue of Neurotin to give rise to a bicyclic lactam **31**, thus showcasing the potential utility of our method in a fine chemical industry.

The obtained chiral γ-lactams could be further transformed to a number of important scaffolds with biological relevance. Representative lactam **2** (98:2 e.r.), which was obtained from a large-scale reaction, was successfully converted to give chiral *N*-arylated lactam **32**, thioamide **33**, chiral pyrrolidine **34** and non-natural γ-amino acid **35** without erosion of enantiopurity. These synthetic derivatives serve as important pharmacophores, as illustrated in Fig. 5.

Conclusions

We have introduced an iridium-based catalyst system for asymmetric C–H amidation that enables facile construction of chiral γ-lactams starting from commodity chemicals such as carboxylic acid

derivatives. A series of Cp*Ir-based catalysts were tested on the basis of mechanistic considerations, and chiral diamines were discovered to be excellent ligand scaffolds for this asymmetric transformation. A wide range of dioxazolone substrates, easily prepared in two steps from the corresponding carboxylic acids, were successfully applied to furnish γ-lactam products in high product yields with excellent enantioselectivity. Various types of secondary C–H bond, for example positioned at the benzylic, unactivated aliphatic, propargylic and allylic sites, were all smoothly reacted in a regio- and stereoselective manner. Extension of the current protocol to desymmetrization of *meso*-substrates was also achieved with excellent enantioselectivity to introduce two consecutive stereogenic centres in a single transformation. To understand the key factors for achieving such high enantioselectivity, computational evaluations of the plausible pathways were performed, which identified a unique hydrogen bonding between the substrate and catalyst that might play a pivotal role in the enantioselectivity-determining process. This computationally guided insight led us to carry out further experimental elaboration to confirm the importance of the hydorgen bond during catalysis. In particular, structural analogues of the highly reactive Ir–carbonylnitrenoid intermediate were successfully synthesized, and spectroscopic signatures of the hydrogen bonding were unambiguously observed. Consistent with this rationale, significant erosion in enantioselectivity was observed when the degree of the hydrogen bond interaction was weakened by the catalyst modification. We anticipate that the present approach will find broad applications in synthetic and medicinal chemistry, and the mechanistic insights may provoke further developments in related asymmetric catalysis.

Methods

Preparation of Ir3, and Ir5 to Ir10. $[Cp^*IrCl_2]_2$ (200 mg, 0.25 mmol), ligand (0.50 mmol) and triethylamine (101 mg, 1.00 mmol) in dichloromethane (10 ml) were stirred for 30 min at room temperature. After completion, the crude mixture was purified by flash chromatography (eluent: CH_2Cl_2/MeOH = 20:1) to afford the desired complexes.

Preparation of Ir12 and Ir13. Organic amide (0.072 mmol) and **Ir11** (50 mg, 0.072 mmol) in dichloromethane (2 ml) were stirred at 50 °C for 15 min. After completion, the solvent was removed under reduced pressure to afford analytically pure product. Further slow diffusion of pentane into saturated solution in chloroform at −30 °C gave fine yellow crystals for X-ray analysis.

Preparation of 3-substituted 1,4,2-dioxazol-5-ones. To a stirred solution of hydoxamic acid (5.0 mmol) in dichloromethane (50 ml) was added 1,1′-carbonyldiimidazole (0.81 g, 5.0 mmol) in one portion at room temperature. After stirring for 30 min, the reaction mixture was quenched with 1 N HCl (30 ml), extracted with dichloromethane three times (50 ml ×3) and dried over $MgSO_4$. The solvent was removed under reduced pressure. The crude mixture was filtered through a pad of silica and washed with dichloromethane. The filtrate was concentrated under reduced pressure to afford 3-substituted 1,4,2-dioxazol-5-ones[28].

General procedure for Ir-catalysed enantioselective C–H amidation reaction. To a 4 ml reaction vial were added **Ir10** (8.1 mg, 5 mol%), $NaBAr^F_4$ (8.9 mg, 5 mol%), anhydrous TCE (0.4 ml), which were stirred with a magnetic stir bar under an Ar atmosphere. To another vial were added 1,4,2-dioxazol-5-one (0.2 mmol) and TCE (0.2 ml). After stirring for 5 min at room temperature, the substrate solution was transferred to the reaction vial, and an additional 0.4 ml of TCE (0.2 ml ×2) was used to ensure complete transfer. The reaction mixture was vigorously stirred in a pre-heated aluminium block at 35 °C for 24 h. After completion, solvent was removed under reduced pressure, and the desired product was obtained by flash chromatography (eluent: *n*-hexane/10% methanol in EtOAc, 4:1).

Procedure for the large-scale reaction. To a 50 ml round-bottom flask were added **Ir10** (65 mg, 4 mol%), $NaBAr^F_4$ (71 mg, 4 mol%) and anhydrous TCE (10 ml) under an Ar atmosphere. After stirring for 5 min at room temperatures, **1** (2.0 mmol, 410 mg) was directly added, and the reaction mixture was vigorously stirred in a pre-heated oil bath at 50 °C for 24 h. After completion, solvent was removed under reduced pressure, and the desired product was obtained by silica chromatography (eluent: *n*-hexane/10% methanol in EtOAc solution, 4:1). A product yield of 94% and e.r. of 98:2 were obtained.

Full experimental details, characterization of new compounds and computational details are provided in the Supplementary Methods.

Data availability

The X-ray crystallographic coordinates for the structures reported in this study have been deposited at the Cambridge Crystallographic Data Centre (CCDC), under deposition nos. 1873622–1873624 and 1884674. These data can be obtained free of charge from The Cambridge Crystallographic Data Centre via www.ccdc.cam.ac.uk/data_request/cif. All other data are available from the authors upon reasonable request.

Received: 5 November 2018; Accepted: 9 January 2019;
Published online: 18 February 2019

References

1. Fisher, J. F., Meroueh, S. O. & Mobashery, S. Bacterial resistance to β-lactam antibiotics: compelling opportunism, compelling opportunity. *Chem. Rev.* **105**, 395–424 (2005).
2. Caruano, J., Muccioli, G. G. & Robiette, R. Biologically active γ-lactams: synthesis and natural sources. *Org. Biomol. Chem.* **14**, 10134–10156 (2016).
3. Ye, L.-W., Shu, C. & Gagosz, F. Recent progress towards transition metal-catalyzed synthesis of γ-lactams. *Org. Biomol. Chem.* **12**, 1833–1845 (2014).
4. Ye, J., Kalvet, I., Schoenebeck, F. & Rovis, T. Direct α-alkylation of primary aliphatic amines enabled by CO_2 and electrostatics. *Nat. Chem.* **10**, 1037–1041 (2018).
5. Png, Z. M., Cabrera-Pardo, J. R., Peiró Cadahía, J. & Gaunt, M. J. Diastereoselective C–H carbonylative annulation of aliphatic amines: a rapid route to functionalized γ-lactams. *Chem. Sci.* **9**, 7628–7633 (2018).
6. Danishefsky, S., Berman, E., Clizbe, L. A. & Hirama, M. A simple synthesis of L-γ-carboxyglutamate and derivatives thereof. *J. Am. Chem. Soc.* **101**, 4385–4386 (1979).
7. Seki, T., Tanaka, S. & Kitamura, M. Enantioselective synthesis of pyrrolidine-, piperidine-, and azepane-type *N*-heterocycles with α-alkenyl substitution: the CpRu-catalyzed dehydrative intramolecular *N*-allylation approach. *Org. Lett.* **14**, 608–611 (2012).
8. Yuan, Q., Liu, D. & Zhang, W. Iridium-catalyzed asymmetric hydrogenation of β,γ-unsaturated γ-lactams: scope and mechanistic studies. *Org. Lett.* **19**, 1144–1147 (2017).
9. Tahara, Y.-k, Michino, M., Ito, M., Kanyiva, K. S. & Shibata, T. Enantioselective sp^3 C–H alkylation of γ-butyrolactam by a chiral Ir(I) catalyst for the synthesis of 4-substituted γ-amino acids. *Chem. Commun.* **51**, 16660–16663 (2015).
10. Gensch, T., Hopkinson, M. N., Glorius, F. & Wencel-Delord, J. Mild metal-catalyzed C–H activation: examples and concepts. *Chem. Soc. Rev.* **45**, 2900–2936 (2016).
11. Davies, H. M. L. & Morton, D. Recent advances in C–H functionalization. *J. Org. Chem.* **81**, 343–350 (2016).
12. Roizen, J. L., Harvey, M. E. & Du Bois, J. Metal-catalyzed nitrogen-atom transfer methods for the oxidation of aliphatic C–H bonds. *Acc. Chem. Res.* **45**, 911–922 (2012).
13. Park, Y., Kim, Y. & Chang, S. Transition metal-catalyzed C–H amination: scope, mechanism, and applications. *Chem. Rev.* **117**, 9247–9301 (2017).
14. Liang, J.-L., Yuan, S.-X., Huang, J.-S., Yu, W.-Y. & Che, C.-M. Highly diastereo- and enantioselective intramolecular amidation of saturated C–H bonds catalyzed by ruthenium porphyrins. *Angew. Chem. Int. Ed.* **41**, 3465–3468 (2002).
15. Reddy, R. P. & Davies, H. M. L. Dirhodium tetracarboxylates derived from adamantylglycine as chiral catalysts for enantioselective C–H aminations. *Org. Lett.* **8**, 5013–5016 (2006).
16. Zalatan, D. N. & Du Bois, J. A chiral rhodium carboxamidate catalyst for enantioselective C–H amination. *J. Am. Chem. Soc.* **130**, 9220–9221 (2008).
17. Milczek, E., Boudet, N. & Blakey, S. Enantioselective C–H amination using cationic ruthenium(II)–pybox catalysts. *Angew. Chem. Int. Ed.* **47**, 6825–6828 (2008).
18. Ichinose, M. et al. Enantioselective intramolecular benzylic C–H bond amination: efficient synthesis of optically active benzosultams. *Angew. Chem. Int. Ed.* **50**, 9884–9887 (2011).
19. McIntosh, J. A. et al. Enantioselective intramolecular C–H amination catalyzed by engineered cytochrome P450 enzymes in vitro and in vivo. *Angew. Chem. Int. Ed.* **52**, 9309–9312 (2013).
20. Dydio, P., Key, H. M., Hayashi, H., Clark, D. S. & Hartwig, J. F. Chemoselective, enzymatic C–H bond amination catalyzed by a cytochrome P450 containing an Ir(Me)–PIX cofactor. *J. Am. Chem. Soc.* **139**, 1750–1753 (2017).
21. Prier, C. K., Zhang, R. K., Buller, A. R., Brinkmann-Chen, S. & Arnold, F. H. Enantioselective, intermolecular benzylic C–H amination catalysed by an engineered iron-haem enzyme. *Nat. Chem.* **9**, 629–634 (2017).
22. Li, C. et al. Catalytic radical process for enantioselective amination of C(sp^3)–H bonds. *Angew. Chem. Int. Ed.* **57**, 16837–16841 (2018).
23. Liang, C. et al. Efficient diastereoselective intermolecular rhodium-catalyzed C–H amination. *Angew. Chem. Int. Ed.* **45**, 4641–4644 (2006).

24. Nishioka, Y., Uchida, T. & Katsuki, T. Enantio- and regioselective intermolecular benzylic and allylic C–H bond amination. *Angew. Chem. Int. Ed.* **52**, 1739–1742 (2013).
25. Pinho e Melo, T. N. V. D. in *Organic Azides: Syntheses and Applications* (eds Bräse, S. & Banert, K.) Ch. 3 (Wiley, New York, 2010).
26. Lebel, H. & Leogane, O. Boc-protected amines via a mild and efficient one-pot Curtius rearrangement. *Org. Lett.* **7**, 4107–4110 (2005).
27. Li, D., Wu, T., Liang, K. & Xia, C. Curtius-like rearrangement of an iron–nitrenoid complex and application in biomimetic synthesis of bisindolylmethanes. *Org. Lett.* **18**, 2228–2231 (2016).
28. Park, Y., Park, K. T., Kim, J. G. & Chang, S. Mechanistic studies on the Rh(III)-mediated amido transfer process leading to robust C–H amination with a new type of amidating reagent. *J. Am. Chem. Soc.* **137**, 4534–4542 (2015).
29. Park, Y., Jee, S., Kim, J. G. & Chang, S. Study of sustainability and scalability in the Cp*Rh(III)-catalyzed direct C–H amidation with 1,4,2-dioxazol-5-ones. *Org. Process Res. Dev.* **19**, 1024–1029 (2015).
30. Park, Y., Heo, J., Baik, M.-H. & Chang, S. Why is the Ir(III)-mediated amido transfer much faster than the Rh(III)-mediated reaction? A combined experimental and computational study. *J. Am. Chem. Soc.* **138**, 14020–14029 (2016).
31. Hwang, Y., Park, Y. & Chang, S. Mechanism-driven approach to develop a mild and versatile C–H amidation through Ir^{III} catalysis. *Chem. Eur. J.* **23**, 11147–11152 (2017).
32. Hong, S. Y. et al. Selective formation of γ-lactams via C–H amidation enabled by tailored iridium catalysts. *Science* **359**, 1016–1021 (2018).
33. Hennessy, E. T. & Betley, T. A. Complex N-heterocycle synthesis via iron-catalyzed, direct C–H bond amination. *Science* **340**, 591–595 (2013).
34. Murata, K., Ikariya, T. & Noyori, R. New chiral rhodium and iridium complexes with chiral diamine ligands for asymmetric transfer hydrogenation of aromatic ketones. *J. Org. Chem.* **64**, 2186–2187 (1999).
35. Camps, P. et al. Synthesis and absolute configuration of novel *N*,*O*-psiconucleosides using (*R*)-*N*-phenylpantolactam as a resolution agent. *J. Org. Chem.* **73**, 6657–6665 (2008).
36. Heiden, Z. M., Gorecki, B. J. & Rauchfuss, T. B. Lewis base adducts derived from transfer hydrogenation catalysts: scope and selectivity. *Organometallics* **27**, 1542–1549 (2008).
37. Koike, T. & Ikariya, T. Mechanistic aspects of formation of chiral ruthenium hydride complexes from 16-electron ruthenium amide complexes and formic acid: facile reversible decarboxylation and carboxylation. *Adv. Synth. Catal.* **346**, 37–41 (2004).
38. Muñiz, K. et al. Metal-ligand bifunctional activation and transfer of N–H bonds. *Chem. Commun.* **47**, 4911–4913 (2011).
39. Jeffrey, G. A. & Takagi, S. Hydrogen-bond structure in carbohydrate crystals. *Acc. Chem. Res.* **11**, 264–270 (1978).
40. Soni, R. et al. The importance of the N–H bond in Ru/TsDPEN complexes for asymmetric transfer hydrogenation of ketones and imines. *Org. Biomol. Chem.* **9**, 3290–3294 (2011).
41. Flack, H. D. & Bernardinelli, G. The use of X-ray crystallography to determine absolute configuration. *Chirality* **20**, 681–690 (2008).
42. Liang, J.-L., Yuan, S.-X., Huang, J.-S. & Che, C.-M. Intramolecular C–N bond formation reactions catalyzed by ruthenium porphyrins: amidation of sulfamate esters and aziridination of unsaturated sulfonamides. *J. Org. Chem.* **69**, 3610–3619 (2004).
43. Saint-Denis, T. G., Zhu, R.-Y., Chen, G., Wu, Q.-F. & Yu, J.-Q. Enantioselective C(sp^3)–H bond activation by chiral transition metal catalysts. *Science* **359**, eaao4798 (2018).

Acknowledgements

This research was supported by the Institute for Basic Science (IBS-R010-D1) in Korea. The authors thank D. Kim (Institute for Basic Science) for X-ray analysis.

Author contributions

Y.P. and S.C. conceived and designed the project and wrote the manuscript. Y.P. carried out the experiments and DFT calculations. S.C. organized the research. Both authors analysed the data, discussed the results and commented on the manuscript.

Competing interests

Y.P. and S.C. are inventors on a patent application no. KR10–2018–0174064, submitted by IBS and KAIST, which covers the preparation and application of the related transition metal catalysts.

Additional information

Supplementary information is available for this paper at https://doi.org/10.1038/s41929-019-0230-x.

Reprints and permissions information is available at www.nature.com/reprints.

Correspondence and requests for materials should be addressed to S.C.

Publisher's note: Springer Nature remains neutral with regard to jurisdictional claims in published maps and institutional affiliations.